A&A 659, A200 (2022)
https://doi.org/10.1051/0004-6361/202142674

Astronomy & Astrophysics

The *Gaia*-ESO Survey: Target selection of open cluster stars⋆

A. Bragaglia[1], E. J. Alfaro[2], E. Flaccomio[3], R. Blomme[4], P. Donati[1], M. Costado[5], F. Damiani[3], E. Franciosini[6], L. Prisinzano[3], S. Randich[6], E. D. Friel[7], D. Hatztidimitriou[8], A. Vallenari[9], A. Spagna[10], L. Balaguer-Nunez[11], R. Bonito[3], T. Cantat Gaudin[11], L. Casamiquela[12], R. D. Jeffries[13], C. Jordi[14], L. Magrini[6], J. E. Drew[15], R. J. Jackson[13], U. Abbas[9], M. Caramazza[16], C. Hayes[17], F. M. Jiménez-Esteban[18], P. Re Fiorentin[9], N. Wright[13], A. Bayo[19], T. Bensby[20], M. Bergemann[21], G. Gilmore[22], A. Gonneau[22], U. Heiter[23], A. Hourihane[22], E. Pancino[6,24], G. Sacco[6], R. Smiljanic[25], S. Zaggia[9], and J. S. Vink[26]

(Affiliations can be found after the references)

Received 16 November 2021 / Accepted 17 December 2021

ABSTRACT

Context. The *Gaia*-ESO Survey (GES) is a public, high-resolution spectroscopic survey, conducted with the multi-object spectrograph Fibre Large Array Multi Element Spectrograph (FLAMES) on the Very Large Telescope (European Southern Observatory, ESO, Cerro Paranal, Chile) from December 2011 to January 2018. *Gaia*-ESO has targeted all the main stellar components of the Milky Way, including thin and thick disc, bulge, and halo. In particular, a large sample of open clusters has been observed, from very young ones, just out of the embedded phase, to very old ones.
Aims. The different kinds of clusters and stars targeted in them are useful to reach the main science goals of the open cluster part of GES, which are the study of the open cluster structure and dynamics, the use of open clusters to constrain and improve stellar evolution models, and the definition of Galactic disc properties (e.g., metallicity distribution).
Methods. The *Gaia*-ESO Survey is organised in 19 working groups (WGs), each one being responsible for a task. We describe here the work of three of them, one in charge of the selection of the targets within each cluster or association (WG4), one responsible for defining the most probable candidate member stars (WG1), and another one in charge of the preparation of the observations (WG6). As the entire GES has been conducted before the second *Gaia* data release, we could not make use of the *Gaia* astrometry to define cluster member candidates. We made use of public and private photometry to select the stars to be observed with FLAMES, once brought on a common astrometric system (the one defined by 2MASS). Candidate target selection was based on ground-based proper motions, radial velocities, and X-ray properties when appropriate, for example, and it was mostly used to define the position of the clusters' evolutionary sequences in the colour-magnitude diagrams. Targets for GIRAFFE were then selected near the sequences in an unbiased way. We used known information on membership, when available, only for the few stars to be observed with UVES.
Results. We collected spectra for 62 confirmed clusters in the main observing campaign (and a few more clusters were taken from the ESO archive). Among them are very young clusters, where the main targets are pre-main sequence stars, clusters with very hot and massive stars currently on the main sequence, intermediate-age and old clusters where evolved stars are the main targets. Our strategy of making the selection of targets as inclusive and unbiased as possible and of observing a significant and representative fraction of all possible targets permitted us to collect the largest, most accurate, and most homogeneous spectroscopic data set on open star clusters ever achieved.

Key words. surveys – stars: abundances – stars: kinematics and dynamics – open clusters and associations: general – techniques: radial velocities – techniques: spectroscopic

1. Introduction

The *Gaia*-ESO Survey (GES, Gilmore et al. 2012, 2021; Randich et al. 2013, 2021) is a large, public spectroscopic survey using the Fibre Large Array Multi Element Spectrograph (FLAMES)[1] instrument (Pasquini et al. 2002) on the European Southern Observatory (ESO) Very Large Telescope (VLT-UT2) to obtain intermediate and high-resolution spectroscopy of $\sim 10^5$ stars in our Galaxy. The observations were conducted in the December 2011-January 2018 period, employing 340 nights. The goal of the *Gaia*-ESO Survey is to quantify the kinematical and chemical abundance distributions of the different components of the Milky Way, including the bulge, thin and thick discs, halo, and a large sample of open clusters (OCs) that sample cluster age, mass, and distance well. We deal with open clusters in the present paper. Coming before the *Gaia* mission results, the stars observed by *Gaia*-ESO were selected making use of several photometric sources, such as the VISTA Hemisphere Survey (VHS, McMahon 2012), the Skymapper project (Keller et al. 2007), and a variety of photometric data for OCs (see below).

As indicated by its name, *Gaia*-ESO intends to complement the data from the *Gaia* satellite[2] (e.g., Mignard 2005; Gaia Collaboration 2016a), which was launched on December 2013. *Gaia* is providing photometry, parallaxes, and proper motions of exquisite quality for more than 1.5 billion objects, that is about 1% of the Galactic stellar population. The first *Gaia* data release (GDR1) happened on September 14, 2016 and contained information on the first 14 months of operation (e.g., Gaia Collaboration 2016b). In GDR1 only positions and *G* band photometry was released for about 1 billion sources. In addition, GDR1 provided parallaxes and mean proper motions for about 2

⋆ Based on data obtained with the European Southern Observatory telescopes under program 188.B-3002 (The *Gaia*-ESO Public Spectroscopic Survey).

[1] FLAMES feeds two spectrographs, the high-resolution UVES and the low and intermediate-resolution GIRAFFE.

[2] https://www.cosmos.esa.int/web/gaia/

Article published by EDP Sciences

million bright stars in common with the HIPPARCOS and *Tycho*-2 catalogues – a realisation of the *Tycho-Gaia* Astrometric Solution (TGAS). Although still limited, GDR1 was used widely by the astronomic community and showed encouraging possibilities for open cluster studies, see for instance Gaia Collaboration (2017) on TGAS astrometry of nearby clusters and a *Gaia*-ESO paper (Randich et al. 2018) combining TGAS and *Gaia*-ESO data to improve the derivation of ages and comparison of stellar evolutionary models.

Gaia DR2 (Gaia Collaboration 2018b), published on April 25, 2018, contained positions, parallaxes, and proper motions for about 1.3 billion sources, together with photometry in G (330–1050 nm), G_{BP} (330–680 nm), and G_{RP} (630–1050 nm) bands and radial velocities (RVs) for about 7 million sources (Sartoretti et al. 2018). This catalogue brought about a revolution in Galactic studies (see Gaia Collaboration 2018a, to cite only one paper on Hertsprung Russell diagrams) and made possible a more detailed analysis of the general OC population and of membership in individual clusters, including new clusters discovered and candidate clusters removed, see for instance Cantat-Gaudin et al. (2018), Liu & Pang (2019), Sim et al. (2019), and Castro-Ginard et al. (2020).

The third data release of *Gaia* has been divided in two parts, and on December 3, 2020, EDR3 (i.e. early data release 3), published updated and more precise positions, parallaxes, proper motions, and photometry (Gaia Collaboration 2021), while the complete DR3, expected in the first half of 2022, will also comprise BP and RP spectra, classification and astrophysical parameters, etc[3]. *Gaia* EDR3 has already been used to derive properties of stellar clusters (e.g., Jadhav et al. 2021, to cite only a case involving other space data, from the UVIT satellite) and we expect a flourishing of studies larger than for DR2, especially once the full release will be available.

The *Gaia* mission is also collecting spectroscopic observations with the RVS (Radial Velocity Spectrometer) at resolution $R \sim 11\,500$ in a region near the Calcium II triplet (845–872 nm) to a limiting magnitude of $G_{\rm RVS} = 16$. The final *Gaia* DR is expected to provide RVs for about 150 million stars, with a precision strongly dependent on spectral type and magnitude. Only for the brighter stars will atmospheric parameters and element abundances be derived (for about five million stars brighter than 12, and two million stars brighter than 11, respectively). *Gaia* DR2 contained RVs for about 5 million FGK type stars down to $G_{\rm RVS} = 12$. For instance, Soubiran et al. (2018) used them to study the Galactic OC population; they were able to recover information on about 8000 stars in about 860 clusters, however, only 50% of them had RV for at least three stars and 35% had only one candidate member. *Gaia* DR3 will increase the sample to a few tens of millions stars.

While very useful, this means that there is a strong need for ground-based spectroscopic observations reaching fainter limits, at higher spectral resolution, and which can provide precise RVs and abundances. The *Gaia*-ESO Survey will supplement the *Gaia* RVS data for a significant subset of *Gaia* targets, so that *Gaia*-precision astrometry can be coupled with *Gaia*-ESO-precision RVs and chemical abundances.

A large fraction of the *Gaia*-ESO programme is dedicated to the study of a large sample of OCs. The top-level scientific goals of the cluster component of *Gaia*-ESO are described in Randich et al. (2021) and what follows is a brief summary.

[3] See https://www.cosmos.esa.int/web/gaia/release for details.

Firstly, we propose to understand how clusters form, evolve, and eventually dissolve and disperse, through the investigation of internal cluster kinematics and dynamics. In fact, clusters may contribute most of the stars of the Milky Way field and are valuable tools for the study of the formation and evolution of the Galactic disc.

Secondly, we intend to pursue the calibration of the complex physics involved in stellar evolution, using clusters as templates at different age, mass, and chemical composition. In fact, to a first approximation, OCs are observational isochrones.

Thirdly, we aim at obtaining the detailed study of the properties and evolution of the Milky Way thin disc. This is achieved through the study of the distribution of chemical abundances and of their evolution with time.

The FLAMES spectra allow us to determine RVs for all observed stars; this permits the identification of true cluster members in all evolutionary phases, from the pre-main sequence (PMS) to the evolved giants, to be used as observational templates for stellar evolution theory. In nearby clusters (within about 1.5 kpc, Jackson et al. 2015) the precision reached in RV (down to 0.25 km s^{-1}) is sufficient to resolve the internal velocity dispersion and give a measure of the internal kinematics (see e.g., Jeffries et al. 2014). This is especially important when coupled with the precise positions, distance, and proper motions from the *Gaia* satellite (see e.g., Wright et al. 2019, the first paper to combine *Gaia*-ESO RVs and *Gaia* PMs for a large-scale kinematic study of a young cluster). The *Gaia*-ESO spectra also provide metallicity and detailed chemical abundances for OCs that sample cluster age, mass, position, and distance well. Those data are fundamental for the study of the metallicity distribution in the disc and its evolution with time, thus providing key input to the chemical evolution models of the Milky Way disc.

A detailed description of the survey, of its goals and methods can be found in the papers by Gilmore et al. (2021) and Randich et al. (2021). We recall here that the *Gaia*-ESO observations are obtained with both the GIRAFFE spectrograph (about 130 fibres, with resolution $R \sim 15\,000$–$25\,000$, depending on the setup used, with a wavelength coverage of a few tens of nm), and the UVES spectrograph (6 or 8 fibres, depending on the setup, with $R \simeq 47\,000$, and covering about 200 nm). Table 1 gives a summary of the gratings used, their characteristics, the kind of clusters (and stars within clusters) that are observed with them, and the most important lines and elements visible with each setup. Some OCs, used as calibrators, were also observed with the same setups of the field stars (HR10, HR21) of the Galactic survey; for them, the selection of stars followed a different method and details can be found in Pancino et al. (2017).

We focus here on the target selection process for the open clusters and on the observation's preparation. In particular, Sects. 2 and 3 briefly describe the selection of clusters and the kind of stars targeted in each cluster, respectively. Section 4 deals with the creation of the catalogues of stars to observe. Section 5 presents the work-flow of the process and the actual preparation of observations. A discussion on the fraction of actual members observed, based also on posterior *Gaia* data, is done in Sect. 6. A short summary is given in Sect. 7.

2. The selection of clusters

To reach the top-level science goals mentioned above, the *Gaia*-ESO Survey targets a very large sample of clusters, covering the whole age-metallicity-mass-Galactic location-density parameter space. Within each cluster, we observe a large and unbiased

Table 1. Setups used for GIRAFFE and UVES observation of open clusters.

Setup	$\lambda\lambda$ (nm)	$R1$	$R2$	No fibres	Stars and clusters on which the setup is mainly used	Prominent lines and elements
			UVES			
520	414-621	47000		6	early type stars	Hγ,β; and see below the case of blue setups
580	476-684	47000		8	late type stars	Hα; Fe I, II; Fe-peak; α-el.; Na; [O I]; Al; n-capt.; Li
			GIRAFFE			
HR03	403.3-420.1	24800	31400	130	early-type st., massive young cl.	Hδ; He I; Si II; IV; O II; [Si II]
HR04	418.8-439.2		24000	130	early-type st., massive young cl.	Hγ; He I; He II; Si IV; N II
HR05a	434.0-458.7	18470	20250	130	early-type st., massive young cl.	He I, II, Si III; Mg II; N II; III; O II
HR06	453.8-475.9	20350	24300	130	early-type st., massive young cl.	He I, II; Si IV; C III; N II and N III; O II
HR09b	514.3-535.6	25900	31750	130	early-type st.	Mg b; Fe I, Fe II; Ti II; Cr I, Cr II; S II; Mn II
HR14a	630.8-670.1	17740	18000	130	early-type st., massive young cl.	Hα; He I, II; Si II; C II; Ti I; Ba II; TiO
HR15n	647.0-679.0	17000	19200	130	late-type st., all cl.	Hα; He I,II, Li; Fe I; Ca; Si; Mg; Ti I; Ba II; [S II]; [N II]; TiO; CaH

Notes. $R1$, $R2$ are the resolution before and after the GIRAFFE upgrade in February 2015, respectively (no change for UVES). The HR04 setup was used only after the upgrade. The number of allocated stars are less than the fibres, since some ($\geq$1 for UVES, $\gtrsim$15 for GIRAFFE) are dedicated to sky positions. We define here stars of O, B, and A spectral type as 'early' and stars of F, G, K, and M spectral type as 'late'. We note that some A-type stars have been observed using UVES 580. For a few clusters used as cross-survey calibrators, also HR10 (533.9–561.9 nm) and HR21 (848.4–900.1 nm) exposures of a fraction of the targets are acquired.

sample of stars using the GIRAFFE fibres and a smaller, biased sample of the most likely cluster members using the UVES fibres. While RV, atmospheric parameters, and metallicity are obtained for the entire sample of clusters and targets within them, there are necessarily also some differences in the way categories of clusters are dealt with, due to the large variety of properties among OCs. These differences are reflected in the selection of targets and the choice of the gratings. However, this does not imply divergence of goals; on the contrary, we build on this variety to obtain a comprehensive picture of the open clusters' family and of their importance for understanding the Milky Way.

The full description of the cluster selection will appear in Randich et al. (2021). We recall here only a few concepts, relevant for the target selection within each cluster. We can divide the *Gaia*-ESO clusters into two main classes and two sub-classes each.

Firstly, we have young clusters (age $\leq$ 100 Myr). They may be without or with massive stars (mass $\geq$ 8 $M_{\odot}$).

Secondly, we have intermediate-age and old clusters (age >100 Myr, up to several Gyr[4]). They may be without or with a red clump (RC).

The two groups are about one third and two thirds of all observed clusters (see Table A.1). This rather artificial division is however useful to characterise the kinds of stars that dominate in the observed clusters and what information can be best extracted from each category to fulfil the survey main goals.

1a) Young open clusters, with no or few massive stars. This group, dominated by a late-type population with at most a few early-type stars, includes young clusters and associations just out of the embedded phase and up to an age of 100 Myr. We focus on clusters in the solar vicinity, up to about 1.5 kpc, to enhance the *Gaia* connection and to be able to reach low-mass cluster members (see below). These clusters are crucial systems to understand the ongoing star formation (SF) processes and the recent SF history of the Galaxy. These processes involve stellar and dynamical evolution, chemical enrichment mechanisms, and connection with the surrounding environment. Data from the *Gaia* ESO survey have brought about significant progress in these studies, especially for the low-mass populations of these systems, thanks to different spectroscopic diagnostics. Radial velocities, presence of at least one between strong lithium absorption (indication of youth) and Hα in emission (indication of activity or accretion processes), and gravity-sensitive spectral lines are all effective diagnostic of cluster membership. The main effort, in young clusters and associations, is to obtain a complete and unbiased sample of cluster stars, for which precise RVs -and possibly abundances- are measured; our strategy is then driven by the GIRAFFE observations. By coupling proper motion data from *Gaia* and *Gaia*-ESO accurate RVs, we are able to determine the cluster dynamics.

Comparison of clusters of different age, environment, structure, and morphology will allow us to understand the dynamical evolution with time of such systems. The data can also help to confirm/refute the claims of triggered star formation in some star forming regions (SFR). Finally, the *Gaia*-ESO spectra, especially those obtained with UVES, provide chemical abundance diagnostics, contributing important constraints on the metallicity distribution evolution.

1b) Massive-star young clusters. They complete the cluster parameter space covered by the young clusters; as they are rare, they are necessarily observed also up to much larger distances than clusters discussed in point 1a. We concentrate on studying the population of young, massive, and hot main sequence (MS) stars and their influence on the clusters. The massive stars profoundly affect the evolution of the cluster as they shed large amounts of mass, momentum, and energy (ionising radiation), which may lead to the dispersal of the parental molecular cloud, and hence to the end of the star formation in that cluster (Lada & Lada 2003). Knowledge of the kinematics of the massive stars and, when feasible, of the lower-mass members of the same cluster, is highly relevant to the cluster dynamics. They are also interesting objects in themselves as they put important constraints on stellar evolution models.

In addition, massive stars are important in determining Galactic abundance gradients (Daflon & Cunha 2004). Their high luminosity allows us to cover larger distances in the Galaxy. As they are very young, their abundance values are much closer to the present-day ones. From a comparison between the Galactocentric abundance gradient of young and older clusters one can derive the time evolution of the gradient, leading to a powerful constraint on models of thin disc formation.

[4] About 10% of all OCs observed have age larger than 4 Gyr; while this could be defined intermediate-age, these clusters are usually referred to as old in OC literature.

2) Intermediate-age and old clusters, with or without red clump. The RC is the locus of stars burning He in their core and is visible in clusters older than about 300–400 Myr, in which a (conspicuous) number of stars evolved from the MS are present. The old OCs are valuable tools to study the formation and evolution of the Galactic disc and rare fossils of its past star formation history. The vast majority of stars born in OCs are indeed dispersed into the Galactic field in a relatively short time (e.g., Janes & Phelps 1994, Gieles et al. 2006), and thus old survived clusters are unique relics of the composition of the interstellar medium (ISM) at the epoch of their formation (e.g., Friel 1995). The study of a well defined sample of clusters in terms of age and Galactocentric distance allows us to understand the spatial distribution of elements in the Milky Way disc and to investigate its evolution with time. The main focus for these open clusters is on the determination of precise chemical abundances, so emphasis is on the spectra of the relatively few stars observed with the UVES fibres. The UVES targets are chosen preferentially from stars in the RC when it is present, to ensure the best homogeneity among different clusters, since they are stars in a well constrained evolutionary phase and span a small range in atmospheric parameters. A secondary goal is to define cluster membership using the RVs obtained with the more numerous GIRAFFE fibres. A clean definition of the evolutionary sequences and especially of key features, such as the MS turn-off, the sub-giant branch (SGB), the red giant branch (RGB), and the RC, is fundamental to derive age through fits to theoretical isochrones. In fact, *Gaia* provides us with very precise parallaxes, so distance can be derived, but age can ultimately be obtained only through comparison with theoretical models. Cluster distance is essential to define the radial distribution of metallicity and chemical abundances in the Galaxy, while precise and homogeneous ages are required to investigate the chemical evolution history. Finally, whenever sufficiently cool spectral types are present on the MS, then lithium abundances can be measured also from the more numerous GIRAFFE spectra.

This division among clusters of different types is of course only a scheme, and for instance, internal dynamics can be studied also for old and nearby clusters. Important legacy items are the definition of cluster members, the study of the initial mass function in nearby clusters, of the lithium depletion, and of the chromospheric activity. Finally, *Gaia*-ESO obtains spectra for PMS, MS stars of all mass and spectral types, and evolved giants. This very large sample of stars at all evolutionary phases in clusters of different ages and chemical compositions will give important and stringent constraints to stellar evolutionary models.

3. Targets observed in the different kind of clusters

Before delving into a detailed description of target selection and observation preparation, we briefly recall the role of the WGs involved. All *Gaia*-ESO activities are organised in WGs and cluster stars observation preparation is done by three of them: WG1 (cluster membership analysis, led by E. Alfaro), WG4 (cluster target selection, led by A. Bragaglia), and WG6b (FPOSS/OB[5] generation, led by E. Flaccomio); the WG2 activities (auxiliary data for cluster target selection) were merged with WG1 and WG4. For more details on the WG structure and operations, see Gilmore et al. (2021).

The science goals and immediate objectives, as described in Sects. 1 and 2, drive the star selection in each cluster. The target stars are selected from the colour-magnitude diagrams (CMDs, see Sects. 4 and 5), taking into account both the position of each star with respect to the cluster evolutionary sequences and the distance from the cluster centre (the latter only if the cluster does not fill the entire FLAMES field of view – FoV). The actual description of the targets selection will be detailed in the next section, we concentrate here on the kind of targets we are dealing with.

We remark that the (few) UVES targets are generally selected from the most secure members, on the basis of the available auxiliary information such as previously published RVs, proper motions, X-ray properties, lithium abundance, chromospheric activity, depending on the cluster type. For cases where no such auxiliary information was available, as for instance in 25 Ori, we were forced to observe less secure members. In the case of old clusters, the main targets for UVES are RC stars, while RGB stars have second priority. In intermediate-age clusters, MS stars may be targeted as well. For young clusters, UVES targets are PMS and MS stars. In addition to the main targets, for nearby clusters of all ages we try to observe (also) some MS stars of late spectral type, for completeness and cross comparison with GIRAFFE. The faint magnitude limit for the UVES targets is $V \simeq 16.5$, which is the limit to obtain $S/N \sim 50$ in six to seven hours[6].

The selection of GIRAFFE targets is aimed at observing inclusive and unbiased samples of cluster star candidates rather than only high probability members (see next section). While we aim at a high degree of statistical completeness, only a significant sub-sample of candidate members is observed in very rich or extended clusters, to avoid excessive use of telescope time. Targets are PMS or MS stars (and evolved stars in old OCs, to ensure RV membership determination for stars in all evolutionary phases), with $V \leq 19$, to match the *Gaia* mission good astrometric precision at the faint limit. For instance, in *Gaia* DR2 the median uncertainty in parallax (proper motions) is about 0.04 (0.05) mas yr^{-1} for $G < 14$ mag sources, 0.1 (0.2) mas yr^{-1} at $G = 17$ mag, and 0.7 (1.2) mas yr^{-1} at $G = 20$ mag (Lindegren et al. 2018). These values are already better in EDR3 and their precision will increase in further data releases based on longer time scales or the full mission duration. In some clusters, the faint limit for GIRAFFE targets could be extended to $V \simeq 19.5$ in order to utilise otherwise spare fibres.

According to the division of clusters' type given in Sect. 2, the following kinds of stars are observed:

1a) In young clusters and SFRs without a dominant population of early type stars, the targets for GIRAFFE are late-type (F to M) stars in the magnitude range $12 \leq V \leq 19$, in the PMS or MS phase. They are observed with the setup HR15n (containing Hα and the Li 670.7 nm line, both important diagnostic lines). The UVES targets are chosen in the magnitude range $9 < V < 15$. They are observed with the 580 nm setup if of late spectral type, and with the 520 nm setup if (a few) bright, early-type stars are targeted. If the information is available, the UVES targets are preferentially selected to be slow rotators ($v \sin i < 15$ km s^{-1}) and not strong accretors (dM/d$t < 10^{-10}\,M_{\odot}$ yr^{-1}).

[5] FPOSS means Fibre Positioner Observation Support Software and it is the fibre configuration programme for the preparation of FLAMES observations; OB stands for observing block, that is the set of instructions for observation execution.

[6] The exposure times for UVES and GIRAFFE were decided in order to reach the intended scientific goals in the allotted time, see Randich et al. (2021) for a full justification.

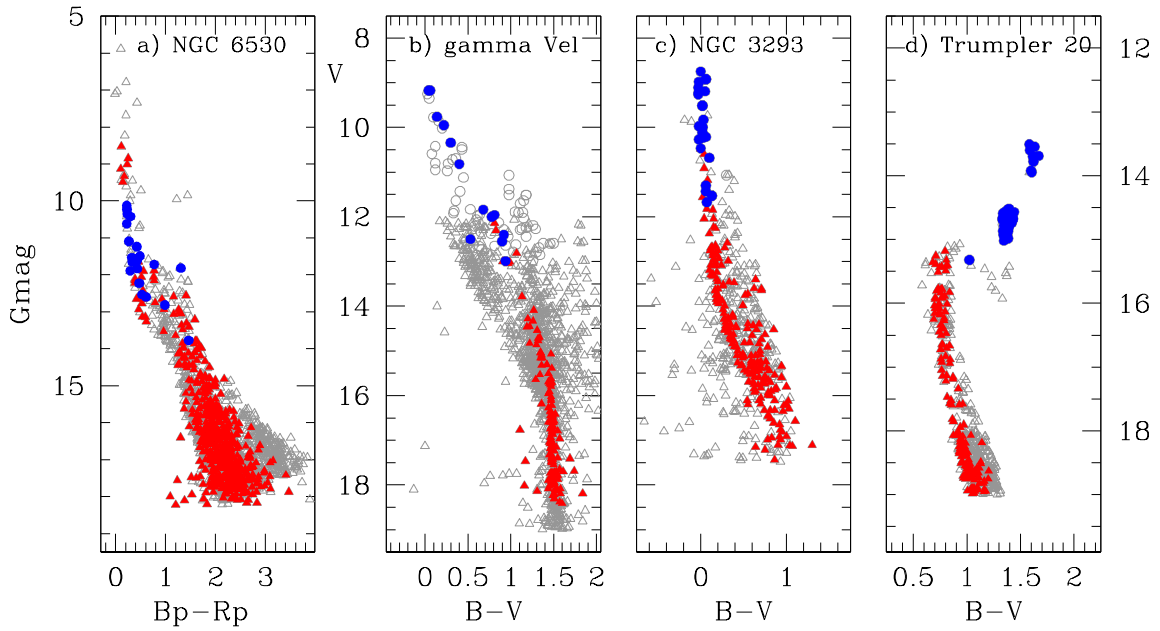

Fig. 1. Examples of targets in four clusters of different ages: (*a*) NGC 6530; (*b*) γ Vel (see text for the numerous field stars), (*c*) NGC 3293, and (*d*) Trumpler 20; their age is about 2 Myr, 20 Myr, 10 Myr, and 1.8 yr (see Table A.1). Open grey symbols indicate all stars observed (triangles GIRAFFE, circles UVES); filled symbols indicate candidate members (red triangles GIRAFFE, blue circles UVES) according to *Gaia*-ESO data.

1b) In young clusters dominated by massive early-type stars, the targets observed with GIRAFFE are B and A-type stars, down to $V \simeq 18$. They are observed with the blue setups HR03, HR04, HR05a, HR06, HR09b, and HR14a (containing Hα). The UVES fibres are allocated to O-type stars in the magnitude range $V = 9-15$ and the 520 nm setup is used.

2a) In old and intermediate-age clusters with RC stars, the GIRAFFE targets are mainly stars from the MS turn-off (TO) down to V= 19. They are observed with HR09b if the spectral type is A to F and with HR15n for later types. Giant stars may also be targeted, with HR15n. Stars observed with UVES (always with the 580 nm setup) are preferentially on the RC. We may also observe RGB stars, as previously mentioned, if the RC is too faint because of distance or extinction, or if there are only a few RC stars. In some nearby clusters, FGK MS stars are also observed with UVES, to compare results with giants. For the UVES targets in the old clusters the magnitude range is $V = 9-16.5$; the fainter limit for these clusters is determined by the requirement to study the metallicity distribution in the disc, hence they are necessarily distributed also out to larger distances.

2b) In intermediate age open clusters without RC stars (i.e. with age between 100 and 300–400 Myr), the target selection is the same as for case *1a)*. The choice of setups for GIRAFFE targets is as for case *2a)*.

3) Whenever possible, a few stars are repeatedly observed in different configurations (e.g., with UVES and GIRAFFE, or in different pointings, or with two or more GIRAFFE setups) to perform sanity checks on the quality of the derived parameters.

These different choices are illustrated in Fig. 1 for four clusters observed early during survey operation, (a) one very young cluster where we targeted both low-mass and early-type stars (NGC 6530, see Prisinzano et al. 2019), (b) one young cluster where we did not target early-type stars (γ Vel, age 5–10 Myr, see Jeffries et al. 2009 and Jeffries et al. 2014, Spina et al. 2014 for first results from the *Gaia*-ESO Survey, or 20 Myr, see Table A.1), (c) one with many massive, early-type stars (NGC 3293, age about 10 Myr, see Baume et al. 2003, Delgado et al. 2007), and (d) one old cluster (Trumpler 20, age about 1.5 Gyr, see for example Carraro et al. 2010 and for first *Gaia*-ESO results, Donati et al. 2014b). In NGC 6530 we targeted almost 2000 stars, of which 55 with UVES 520 nm or 580 nm (for a total of 661 candidate members, see Prisinzano et al. 2019). In γ Vel we observed about 1240 stars with GIRAFFE (135 are candidate members) and 80 stars with UVES (13 are candidate members); in NGC 3293 we observed 540 stars with GIRAFFE (210 members) and 26 with UVES (25 members); in Trumpler 20 we observed 525 stars with GIRAFFE (156 members) and 42 with UVES (41 members). The number of member stars is based on RVs (and other indicators for γ Vel) and is taken from the first analysis of the data; it may vary a little with a more in-deep procedure taking into account, for instance, also the presence of binaries and astrometric information (see Sect. 6), but is accurate enough to illustrate the situation. The apparently low success rate in γ Vel depends on the fact that we preferred to assign fibres to low priority targets rather than leave them unused; even so, the observations brought very interesting results, for instance demonstrating the existence of two sub-groups, γ Vel A and B (Jeffries et al. 2014). In any case, the spectra of field stars may be useful as a legacy, especially now that their distance is known thanks to the *Gaia* satellite results, see e.g., Magrini et al. (2021) and Romano et al. (2021), where field stars observed in the same field as the targeted OC were used to study the lithium distribution and evolution in giant stars.

4. Tailoring a primary list of tentative star targets

As has already been said in the previous sections, the strategies followed for selecting UVES and GIRAFFE targets are very different, since they answer two different questions. The (few) UVES spectra are used to derive the metallicity and detailed abundances and efforts are made to assign the few fibres to the most secure member stars. This means, depending on the cluster type, that we considered auxiliary literature information: RV

and proper motions (for the older clusters) and additionally X-ray properties, lithium abundance, Hα emission, chromospheric activity, and rotation (for the younger clusters and the SFRs). The choice of UVES targets is then strongly biased and will not be discussed anymore in this section.

The (many) GIRAFFE spectra are used to study the general properties of the clusters and the following description applies to the selection of GIRAFFE targets. Since one of the fundamental aspects of the *Gaia*-ESO project is its legacy character, the selection of targets must produce a catalogue representative of a sample as much complete and unbiased as possible, which is also potentially useful and easily accessible to the astronomical community interested in similar scientific objectives or which can be used beyond the original survey goals (this is of course valid also for the UVES spectra). While we aim at reaching a complete coverage of the clusters, practical considerations on the time required force us to limit ourselves to a representative sample. There are three main constraints we considered for tailoring the primary list of target stars.

Firstly, we aim at homogeneity. The procedure has to be as homogeneous as possible even if the data are not and the clusters under study have very different observational characteristics, such as different magnitude ranges, different degrees of field star contamination, different photometric systems, existence of RV data or good-quality proper motions, etc.

Secondly, we require simplicity. The tools used should be easily accessible for anyone, in such a way that the verification and control of the final product can be reproduced by anyone.

Thirdly, we need unbiased samples. Only those stars considered with certainty as non-members should be excluded from the final list (i.e. the evident outliers from the stellar population of the cluster). Although this criterion entails the possible inclusion of (a significant fraction of) field stars, the final list will be more in line with the general objectives of the project and its character as a legacy programme than if we performed a more restrictive purge.

Therefore, for GIRAFFE targets we selected candidate cluster members on the basis of photometry. Other astronomical data were only used to define the spatial extent and the evolutionary sequences for each cluster, along which we picked stars to be observed. Furthermore, proper motions were used, when possible, to exclude a small fraction of potential targets visualised as kinematic outliers (see the description below).

We describe in this section the data sources, the tools, and the kinematical selection of members that helped the final selection. We present details for one cluster as example.

4.1. Data sources

The target selection involves a laborious process of looking for potential sources of optical photometry (and ancillary information on membership). This means that only clusters where there are sufficient photometric data are included in our sample.

Photometry and kinematic information on the cluster sample are the basic ingredients for the target selection. Unfortunately, no single, homogeneous, and all-sky dataset covers all the clusters of the *Gaia*-ESO programme[7], so we resorted to individual available photometric studies. However, the European Galactic Plane Surveys (EGAPS)[8] optical photometry covers part of the cluster sample: IPHAS and UVEX (INT Photometric Hα Survey, Drew et al. 2005, UV-Excess Survey, Groot et al. 2009) in the north and the public ESO survey VPHAS+ (VST Photometric Hα Survey, Drew et al. 2014) in the south. Collectively, these surveys use the Sloan *ugri* broadband filters, and Hα narrow band, achieving a 5σ faint limit >20 in all bands. The bright limit is typically 12–13th magnitude. This suits them well to our selection needs.

Table 2. Summary of main catalogues used in the target selection.

Optical	NIR	PM	Others
EGAPS	2MASS	UCAC4	Li abundance
IPHAS/UVEX		SPM4	X-ray
VPHAS		PPMXL	RV

Individual CCD optical photometric studies were used for some of the clusters; in some cases, they were the only source of targets. The public data were retrieved from the WEBDA[9] database and the VizieR catalogue access tool[10]. In a few cases, specific photometric studies have been performed for selected clusters or archive wide-field images have been analysed. Details on the photometric source(s) are presented in the various *Gaia*-ESO papers on OCs (e.g., Donati et al. 2014a, for Berkeley 81 and S. Zaggia, priv. comm., for NGC 4815 and NGC 6705).

In the near-infrared range, the 2MASS catalogue (Skrutskie et al. 2006) is the main data source. These data are used for membership selection and for establishing an astrometric reference frame for fibre positioning. The 2MASS catalogue, given its all-sky character and its well-proven accurate astrometry (better than 0.1 arcsecond for sky positions), is the basis of our pre-*Gaia* coordinate system.

Several ground-based, large-area proper motion (PM) catalogues have been the source of our 2D kinematic information: the UCAC4 (Fourth US Naval Observatory CCD Astrograph Catalogue, Zacharias et al. 2013), SPM4 (Southern Proper Motion Program IV, Girard et al. 2011), and PPMXL (Positions and Proper Motions-Extended, Röser et al. 2008) catalogues. When available, we used preferentially the UCAC4 all-sky catalogue or the SPM4 PM data. Table 2 gives a summary of the main catalogues and other physical variables involved in the targets' selection; for specific clusters, RV data and other physical information were taken from the ViZieR and WEBDA databases.

Literature data concerning RVs for cluster stars are more sparse, non-homogeneous, and far from complete for the cluster selection. The WEBDA and the catalogues at CDS are the best RV data providers. Also in this case, some effort has been devoted to obtaining new spectra to measure RVs for stars in *Gaia*-ESO clusters (e.g., Hayes & Friel 2013).

Finally, other physical variables, such as metallicity, X-ray emission, Li abundance, and any other information that might help discriminate between cluster members and field stars was used to help define the cluster photometric sequences. In particular, X-ray emission and lithium abundance are useful for young clusters (age less than about 100 Myr) and SFRs. In these cases we identified candidate members based on their young age with respect to older, disc stars. In fact, young stars show X-ray fluxes

[7] We use the Two Micron All Sky Survey (2MASS, Skrutskie et al. 2006), as described in the text, but it does not reach faint enough and with the required precision. Furthermore, *JHK* data alone are insufficient to select a complete sample of cluster members without including far too many non-members.

[8] http://www.ing.iac.es/Astronomy/development/iphas/ http://www.vphasplus.org

[9] http://webda.physics.muni.cz/

[10] https://vizier.cds.unistra.fr/viz-bin/VizieR

significantly larger than those observed in older stars of the same spectral type (e.g., Favata & Micela 2003, Feigelson et al. 2007). Lithium is easily destroyed at relatively low temperatures, starting already in PMS. Thus, presence of high lithium abundance is a well known tracer of youth and indicates a high probability of belonging to the SFR under study (see e.g., the analysis in a few *Gaia*-ESO papers on young clusters: Jeffries et al. 2014, Rigliaco et al. 2016, Sacco et al. 2017, and Wright et al. 2019, all of which rely on the presence of lithium to determine youth for studies of these clusters).

4.2. Tools and procedure

The selection of the candidate cluster members was primarily based upon their position in the CMDs. This means we took into account the expected location of the different evolutionary sequences in the various observational diagrams.

The first step is the definition of the cluster sequences and the spatial extent of the cluster. For this we made use of both the theoretical isochrones that best fit the published physical parameters of the cluster and the location of those stars that have membership information. We used the PARSEC isochrone models (PAdova and TRieste Stellar Evolution Code, Bressan et al. 2012) for the MS and post-MS stars of the clusters in any age range and those calculated by Siess et al. (2000) for the PMS stars.

Then we selected the regions in the CMDs around the cluster main loci. The width of the CMD strip used for selection depends on several factors, such as variable reddening, binary sequence, and photometric errors, but always taking into account that we need to be inclusive. The subjective component of this selection is moderated by the use of multi band photometry, with the possibility of analysing various CMDs to better define the sequences.

The next step was then assigning a new variable to each star, indicating whether it is a candidate member or not, according to its position in the various CMDs, independently in the optical and near-IR bands. The 2MASS photometry does not always reach as deep as the optical one, so the latter is more important for the fainter part of the sequences.

The final step for all clusters for which this is feasible, was the determination of the kinematic outliers. We could only do that when a sample of at least 20 secure members, identified independently, is available. These firmly identified cluster members were cross identified in the PM catalogue. From the selection of 20 or more bona fide cluster members, we estimated the statistical parameters of a 2D Gaussian model of the proper motions of the cluster in such a way that χ^2 is close to 1. To this aim, we considered additional systematic uncertainties $\sigma_{\alpha,\mathrm{sys}}$ and $\sigma_{\delta,\mathrm{sys}}$ with typical values between 1 and 4 mas yr^{-1}, added in quadrature to the PM errors. The fitted proper-motion centroid of the cluster is $(\mu_{\alpha,\circ}, \mu_{\delta,\circ})$. The final selection proceeded keeping a photometric candidate if

$$\sqrt{\frac{(\mu_\alpha - \mu_{\alpha,\circ})^2}{\sigma_\alpha^2 + \sigma_{\alpha,\mathrm{sys}}^2} + \frac{(\mu_\delta - \mu_{\delta,\circ})^2}{\sigma_\delta^2 + \sigma_{\delta,\mathrm{sys}}^2}} < 5$$

or if there is no valid PM information; μ_α, μ_δ, and the corresponding sigma are the PM in right ascension and declination and the associated errors. Finally, we should note that clusters with a number of bona fide kinematic members lower than 20, as well as those clusters without any previous kinematic membership study, were not analysed using this procedure and we had to rely only on the photometric data and isochrones to define possible targets.

We wish to stress that we have a range of cases, from clusters for which it was not possible to apply a kinematic membership analysis and where the separation of candidate members depends entirely on the photometry, to objects with a careful kinematic description and separation between cluster and field stars. We worked with a wide variety of observational samples with different degrees of completeness and bias in the composition of the cluster and field mix. One of the immediate aims of the programme is the evaluation of the quality of candidate member selection, using the RV and abundance data determined by the *Gaia*-ESO Survey and the astrometric information provided by the *Gaia* mission (see Sect. 6, the many *Gaia*-ESO papers, and Randich et al. 2021).

4.3. The case of NGC 6705

To better explain the selection process, we show an example of application of this methodology to NGC 6705, which was observed during the first six months of *Gaia*-ESO operations (May, June 2012). Literature parameters for this cluster are: age = 250 Myr, $(m - M)_0 = 11.55$, $E(B - V) = 0.43$ (see Sung et al. 1999), and [Fe/H] = +0.10 (Gonzalez & Wallerstein 2000). These values are similar to those derived by Cantat-Gaudin et al. (2014), who used the data described below and the first *Gaia*-ESO results. Photometry in the V and B bands for about 22 000 stars within a FoV with side of 22.5′ were taken from Koo et al. (2007). We selected candidate cluster stars, as shown in Fig. 2a, where red dots represent the photometric candidates along the cluster MS, as well as those stars lying on the blue straggler, binary sequence, and RC locations. We did that separately for the optical and near infrared (NIR) CMDs. From the BV selection, we matched the optical photometry with 2MASS data. The infrared analysis was based on the selection of the probable cluster members according to their relative position on the CMDs. The selected candidates are plotted in Fig. 2b, where red dots represent the candidates after the NIR filtering.

Radial velocity measurements for stars in the field of NGC 6705 were secured by Kharchenko et al. (2007), Mermilliod et al. (2008), and Frinchaboy & Majewski (2008). In addition, HARPS data were taken from the ESO archive, originated by the programme 'Search for Planets around Evolved Intermediate-Mass Stars' (Lovis & Mayor 2007). Thus, for our analysis we had a total of 38 bona fide cluster members (indicated in Fig. 2a) with RV and PM measurements (the latter come from the UCAC4 catalogue). This means that we could apply a selection based on kinematic criteria, according to previous section.

The determination of the cluster proper motion parameters was performed following the procedure outlined above, yielding -2.7 ± 0.7 mas yr^{-1} and -2.0 ± 0.5 mas yr^{-1} for the PM cluster centroid[11], with a systematic error of 2.5 mas yr^{-1} and 1.3 mas yr^{-1}, respectively. To apply these values, we matched the optical and infrared selected candidates with the PM catalogue. The selection of the kinematic outliers and possible members of the cluster was made according to these parameters down to $V \sim 17$. We found 226 stars whose proper motions are more than five sigma from the cluster centroid (see Figs. 3 and 2c) and therefore they were excluded from the sample. Thus we selected a total of about 3400 candidate members, of which about 2250 do not have kinematic information.

[11] The cluster average values obtained by Cantat-Gaudin & Anders (2020) are -1.560 ± 0.160 and -4.144 ± 0.161 mas yr^{-1}, respectively, based on more than 1000 stars down to $G = 18$ measured by *Gaia*.

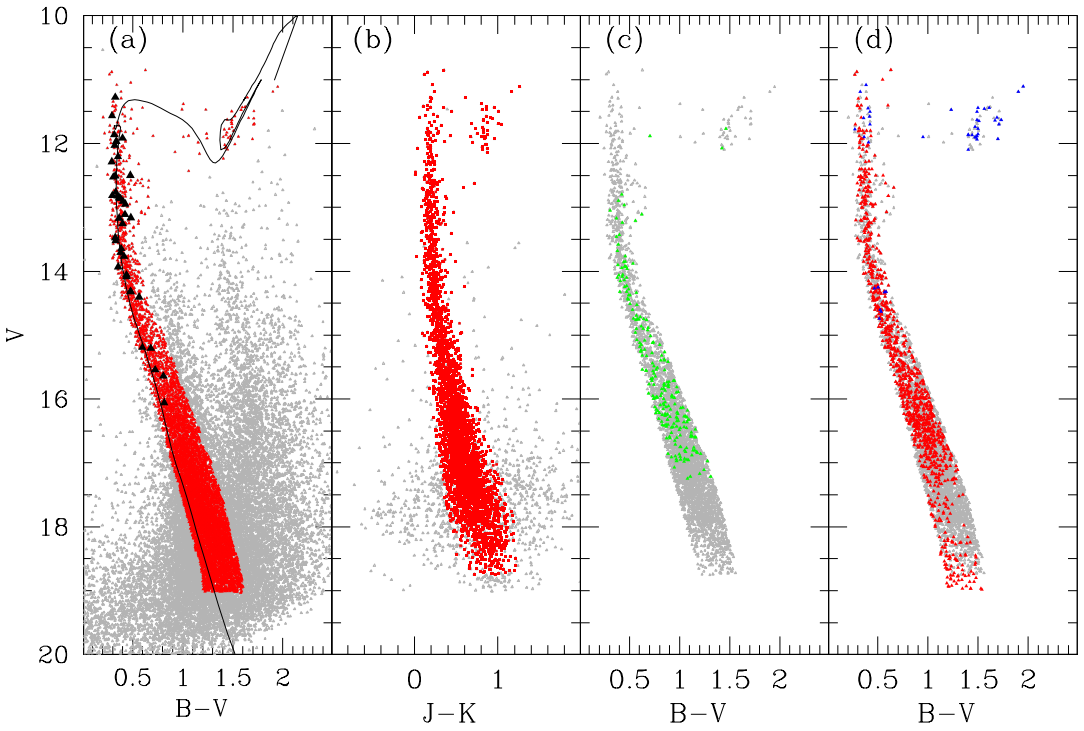

Fig. 2. Step by step procedure (from left to right) applied in the selection of candidate members. (*a*) $V, B-V$ CMD for NGC 6705, showing the selection of candidate members. In grey we show all stars with optical photometry, while red filled triangles represent the stars selected on the basis of *BV* photometric information. The line is the best-fit PARSEC (Bressan et al. 2012) isochrone (see Cantat-Gaudin et al. 2014), while the black symbols are selected members from kinematic analysis (see Sect. 4). (*b*) The stars selected in the optical bands are shown in grey, in the *V* vs. $J-K$ CMD; here red points represent the stars selected based on *JHK* analysis. (*c*) Candidate targets in grey, with kinematic outliers shown in green. (*d*) Final selection (in grey) is shown together with the stars actually observed (in red with GIRAFFE, in blue with UVES fibres).

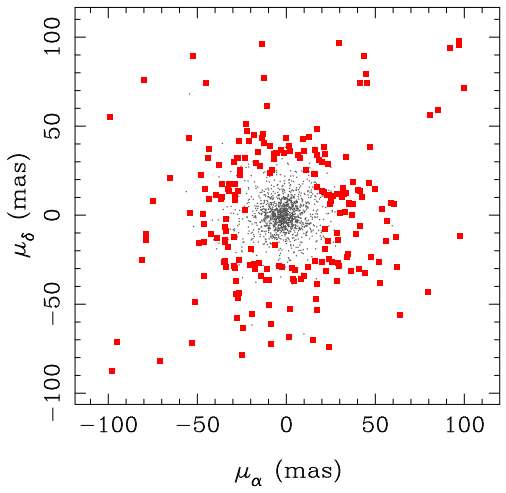

Fig. 3. Proper motion distribution for photometric candidate targets for NGC 6705 (grey symbols). Red filled squares represent kinematic outliers according to the procedure described in the text.

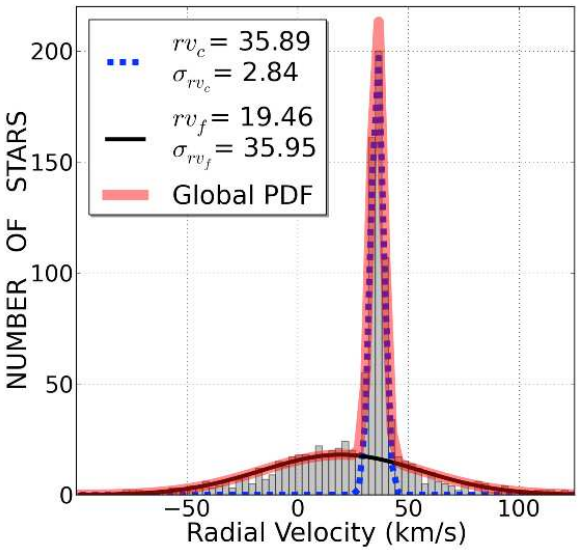

Fig. 4. Distribution of the RVs of the 1028 stars observed with GIRAFFE in NGC 6705. The solid black line and the dashed blue line represent the field stars and cluster members radial velocity distributions. The probability density function (labelled PDF) of the total sample is plotted in red. As can be observed, a mean value of 35.89 km s^{-1} is found for the RV of the cluster members, with a standard deviation of 2.84 km s^{-1}. For the field stars, the mean RV is 19.46 km s^{-1} and the standard deviation 35.95 km s^{-1}.

For this cluster we had additional images in the *B*, *V*, and *I* filters taken with the Wide Field Imager at the Max-Planck-Gesellschaft/ESO 2.2m Telescope for the ESO Imaging Survey (ESO programme 163.O-0741(C), PI Renzini) in a field of 30×30 arcmin^2. These data were reduced as described in Cantat-Gaudin et al. (2014) who present *B*, *V* and *I* photometry for more than 123 000 stars down to $V \sim 22$. This catalogue was used for making the final selection and formed the basis for the preparation of the observing plan.

Of the sample described above, 1028 stars have been observed with GIRAFFE (860 with the HR15n setup and 166 with the blue setups, see Table 1) and 59 with UVES (ten with

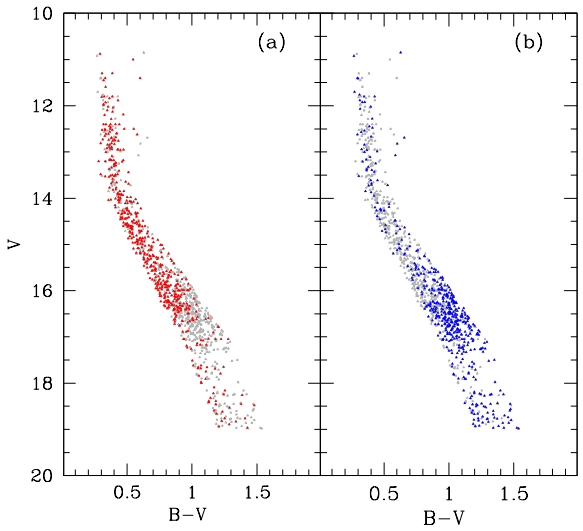

Fig. 5. (*a*) V, $B-V$ CMD for NGC 6705 showing the stars observed with GIRAFFE in grey and RV candidate cluster members in red. (*b*) As in previous panel, but with candidates non members indicated in blue.

Table 3. Summary of exposure times for late type stars.

Setup	mag range	exp. time (min)	S/N (goal)
	Old clusters [a]		
UVES 580/520	$V < 13$	50	>60
	$13.0 < V < 14.5$	3×50	>60
	$15.5 < V < 16.5$	5×50	>60
	$15.5 < V < 16.5$	7×50	>60
GIRAFFE HR09b/15n	$13.0 < V < 15.0$	25	>20
	$15.0 < V < 19.0$	2×50	>20
	SFRs and young clusters [b]		
GIRAFFE HR15n	$12.0 < V < 16.0$	20	>15
	$16.0 < V < 19.0$	50	>15
UVES 580/520	$V < 12.0$	20	>60
	$V < 13.5$	50	>60
	$V < 14.2$	2×50	>60
	$V < 15.2$	3×50	>60

Notes. [a]Exposure times driven by UVES observations. [b]Exposure times driven by GIRAFFE observations.

the setup U520, 49 with U580). These are shown in Fig. 2, panel d, (red and blue dots for Giraffe and UVES, respectively) along with the candidate members of the cluster (grey small dots). Post-observation membership is based here solely on RV values. An analysis of the radial velocity distribution reveals two Gaussian populations whose statistical parameters are presented in Fig. 4 and which lead to 536 stars classified as members of the cluster, representing 52% of the observed population.

Figure 5 shows our results, only for the stars observed with GIRAFFE (since the UVES fibres were generally allocated to stars known to be members); panels a and b display the CMD of stars found to be high probability member and non member, respectively. For a more detailed treatment of this cluster see Cantat-Gaudin et al. (2014).

5. The work-flow of the target selection and OB preparation

The clusters observed, their assigned priority, and the driving science goals which motivated their study are discussed elsewhere (Randich et al. 2021)[12]. We only recall that the clusters have been selected taking into account the available information at the time of observations (essentially January 2012 to January 2018), especially regarding photometry and astrometry. In fact, we require the former to select target stars in the various evolutionary phases and the latter to allocate the FLAMES fibres and produce the so-called OBs, that is the suite of information needed to perform the observation.

We collected all relevant photometric data, including literature sources, private data, and on-going surveys. A large effort was devoted to collecting all existing literature information on the proposed clusters. Their properties and parameters are often rather controversial. The stars were cross-identified to intercompare and combine the photometric sets. We then identified the kind of stars to be observed (see Sect. 3). Unified criteria were used to determine instrumental setups and exposure times on the basis of target spectral type (e.g., late-type dwarf versus early type dwarf), target magnitude, fibre type (GIRAFFE or UVES), and scientific goals (e.g., RV vs. abundances determination).

When possible, we performed a kinematic membership analysis, as described in Sect. 4.2. For the others, the *Gaia*-ESO survey is the first source of kinematical information. Furthermore, the number of observed stars and for which we obtain at least RV data, largely exceeds all existing samples for all clusters.

During the target selection, care was taken to find all ESO archive observations regarding the clusters, especially those containing spectroscopic data. This helped to exclude stars already observed, or to include a sub-sample of them for calibration and testing purposes. Furthermore, all the archive observations compatible with the *Gaia*-ESO goals (similar resolution spectra, wavelength coverage, etc) have been re-analysed homogeneously, to increase the *Gaia*-ESO sample.

To avoid mis-centring of the targets in the fibres, we ensured that the coordinates of all targets, as well as those of auxiliary stars used for guiding and alignments, were on a precise and homogeneous astrometric system. We used coordinates from 2MASS or from other catalogues with better precision, registered to the 2MASS system. All guide and fine-guidance stars were chosen to have possibly low proper motion (even if the observing software can compensate for that). At least 15 GIRAFFE and one UVES fibres were always assigned to sky positions, chosen so to follow as much as possible the spatial distribution of science targets. For fields with strong and spatially variable sky emission (e.g., some SFRs), more GIRAFFE sky fibres were allocated, to improve the subtraction of sky features (see e.g., Bonito et al. 2020).

Once the fibre allocation was done, we prepared binary FITS tables with information on astrometry and photometry for all observed stars (one per each OB), to be added to the reduced files that could be used for the scientific analysis and finally made public through the ESO dedicated archive. The use of FITS tables ensures format uniformity and portability.

Tables 3 and 4 give the exposure times for representative cases of late-type and early-type stars, respectively. All observations, as described by the OBs, were split into two or

[12] For the list of the 62 objects observed by GES, see Table A.1 and Fig. A.1.

Table 4. Summary of exposure times (in min) for early-type stars.

Setup	mag range	Exposure time					
		Original		Revised (Dec 2013)		Revised (Dec 2014)	
		O,early-B	late-B,A	O,early-B	late-B,A	O,early-B	late-B,A
U520	$8 < V < 11$	[a]	[a]	[a]	[a]	[a]	[a]
HR03	$10 < V < 13$	—	—	—	—	36	—
	$11 < V < 14$	34	—	87	—	90	—
	$12 < V < 15$	86	29	*110*	74	*112*	58
	$13 < V < 16$	*107*	73	—	*93*	—	*75*
	$13 < V < 17$	—	*94*	—	—	—	—
HR04, HR05A	$10 < V < 13$	—	—	—	—	13	—
	$11 < V < 14$	17	—	60	—	32	—
	$12 < V < 15$	41	12	*75*	42	*40*	21
	$13 < V < 16$	*51*	31	—	*53*	—	*26*
	$13 < V < 17$	—	*40*	—	—	—	—
HR06	$10 < V < 13$	—	—	—	—	9.3	—
	$11 < V < 14$	14	—	46	—	23	—
	$12 < V < 15$	35	10	*58*	33	*29*	15
	$13 < V < 16$	*43*	25	—	*41*	—	*19*
	$13 < V < 17$	—	*32*	—	*105*	—	*49*
HR09B	$10 < V < 13$	—	—	—	—	15	—
	$11 < V < 14$	32	—	86	—	38	—
	$12 < V < 15$	79	21	*108*	56	*47*	25
	$13 < V < 16$	*99*	54	—	*70*	—	*32*
	$13 < V < 17$	—	*69*	—	—	—	—
HR14A	$10 < V < 13$	—	—	—	—	5.6	—
	$11 < V < 14$	14	—	19	—	14	—
	$12 < V < 15$	34	—	46	—	35	—
	$13 < V < 16$	*42*	22	*57*	30	*44*	23
	$13 < V < 17$	—	*28*	—	*38*	—	*29*

Notes. [a]Exposure times are set by the corresponding exposure times for GIRAFFE. The original exposure times were based on the GIRAFFE exposure time calculator. However, we experienced problems attaining the required S/N and the integration times were increased in December 2013. With the introduction of updated values in the GIRAFFE exposure time calculator, these were again revised in December 2014. The integration times aim for a $S/N > 100$ for O,early B, and >50 for late-B,A spectral types. For fainter stars, we cannot reach these values within a reasonable integration time, so the lower values of $S/N > 70$ and 35, respectively, are aimed for; these integration times are set in italic. See Blomme et al. (2022) for details.

more equal exposures for cosmic rays rejection and to allow for a short exposure with the Th-Ar wavelength calibration lamp on to obtain precise RVs (only five special fibres are illuminated in the *Simcal* observations). Short exposures with the lamp on were interleaved with the science exposures for the following setups: HR09b, HR14a, and HR15n. At the start of the Survey, for HR03, HR04, HR05A, and HR6, the lamp was kept on during the science exposure. As this led to contamination of some of the stellar data, the practice was discontinued (Blomme et al. 2022).

The number of pointings and setups for each cluster, and thus the total observing time, was chosen as to observe a large fraction, ideally >80%, of the candidate cluster members. However, this is difficult to generalise and in most cases impossible to reach. Sometimes photometry is available only on a limited area and does not cover the whole cluster extension. There are limitations due to the instrument itself, such as the FoV of 25′ in diameter and the minimum fibre separation of 10.5″ that makes pointing more difficult in the crowded central regions; we need to assign fibres to enough sky positions to ensure a reasonable background correction (in presence of variable extinction, such as in SFRs, their number and distribution must follow closely that of the stars); and we need to assign fibres to guide stars, which take precedence over targets. Finally, we have only a limited amount of time assigned to each cluster, chosen to balance the sample of clusters and of stars observed in each of them (see Randich et al. 2021).

Given all the above limitations, a lower completeness fraction is acceptable, especially for distant and rich clusters, as well as for the outer parts of spatially extended clusters, when observing so many stars becomes prohibitively time consuming. We can take as a sort of completeness parameter the ratio of possible targets to actually allocated fibres, which varies from about 20 to 80%, with the lower values corresponding generally to the richer, more concentrated clusters (e.g., Trumpler 20, NGC 6705) and the higher to nearby, sparse objects (e.g., γ Vel). The goal is to always observe a representative and significant sample of cluster stars and we deem to have reached it.

6. Actual fraction of member stars observed

To see how *Gaia*-ESO fared in observing cluster members, we may calculate the quotient between confirmed members and observed stars. In Table 5, we report this ratio for a series of clusters already individually analysed, ordered by paper publication date. We take the numbers from the reference papers, indicated

Table 5. Fraction of GIRAFFE members in *Gaia*-ESO clusters already published.

Cluster	Fraction	Ref paper
Trumpler 20	38%	Donati et al. (2014b)
γ Vel	17%	Jeffries et al. (2014)
	19%	Prisinzano et al. (2016)
NGC 4815	29%	Friel et al. (2014)
NGC 6705	52%	Cantat-Gaudin et al. (2014)
Berkeley 81	16%	Magrini et al. (2015)
ρ Oph	15%	Rigliaco et al. (2016)
NGC 3293	24%	Delgado et al. (2016)
Trumpler 23	40%	Overbeek et al. (2017)
NGC 6802	52%	Tang et al. (2017)
Chamaleon I	13%	Sacco et al. (2017)
Carina (Tr14,Tr16,Cr232)	36%	Damiani et al. (2017)
IC 2602	7%	Bravi et al. (2018)
IC 2391	13%	Bravi et al. (2018)
IC 4665	22%	Bravi et al. (2018)
NGC 2547	42%	Bravi et al. (2018)
Pismis 18 [(a)]	18%	Hatzidimitriou et al. (2019)
NGC 2420	61%	Semenova et al. (2020)

Notes. [(a)]For this cluster also *Gaia* DR2 data were used to confirm membership, in addition to RV.

in the table, and use only studies and information related to GIRAFFE observations, since the UVES targets were preselected also on the basis of existing membership data. A caveat is that they relied on early releases and slightly different numbers might come out from analysis based on the final data release and the combination with *Gaia* data (see e.g., Jackson et al. 2020). For intermediate-age and old clusters, the post-observation candidate members were selected based on their photometry and other literature parameters where possible (RV, distance from the cluster centre and a metallicity similar to the bulk of the cluster population) as explained in previous section. For the young clusters, other indicators were generally preferred as more robust, such as lithium abundance (see the original papers for motivation and details). The ratio generally ranges between 15% and 60%, with older clusters having in general a better score. We stress again that contaminants can be (and were) used for science and that in the close-by, young clusters the requirement of being unbiased means we had to accept the possibility of having a large number of contaminants.

We can check a posteriori how well our selection of candidate members fared in observing a representative sample by asking how well we did in comparison with a completely independent selection based on *Gaia* astrometry. Various groups studied OCs with *Gaia* DR1 and especially DR2; one of the more complete samples of OCs and candidate members has been compiled by Cantat-Gaudin et al. (2018) and Cantat-Gaudin & Anders (2020). They provide tables with a membership probability for more than 2000 OCs. Table 6 shows a few examples of a comparison for several clusters contained in a single FLAMES FoV (diameter 25 arcmin) for simplicity. We compare the number of stars observed and candidate members in our survey with the number of high probability members defined only on the basis of *Gaia* astrometry. The columns give: the number of stars actually observed; the number within the same magnitude limit of Cantat-Gaudin et al. (2018), Cantat-Gaudin & Anders (2020), i.e. $G = 18$; the number of stars in a region centred on each cluster with a radius of 12.5 arcmin in the *Gaia*-based catalogue; the numbers of stars with high astrometric membership probability (we choose here 0.7 and 0.9) in the same region; the number of members in each cluster in *Gaia*-ESO according to Jackson et al. (2021, see below); and finally the ratios of *Gaia*-ESO to *Gaia* candidate members. We see that we managed to observe a high fraction of possible members.

Deriving a membership fraction for all clusters is outside the scope of the present paper, as the methods and results depend on the scientific case one wishes to address. However, a more uniform analysis on a large sample of clusters was performed by Jackson et al. (2020, 2021). In the first paper, they used the internal DR5 of *Gaia*-ESO and *Gaia* DR2 and studied the kinematical properties of 32 OCs. They determined the membership probability using a maximum likelihood analysis of the 3D velocity distributions (RV and tangential velocity computed on the basis of proper motions in right ascension and declination plus parallax) in each cluster, taking also into account variations in RV due to binarity. In the second paper, the same kind of analysis was extended to 70 objects in iDR6, 63 open and seven globular clusters (Jackson et al. 2021, note that one of the *Gaia*-ESO targets, Loden 165, was not confirmed to be a real cluster.).

We can compare these results with membership probabilities derived on the basis of parallaxes and proper motions, as in Cantat-Gaudin et al. (2018), Cantat-Gaudin & Anders (2020). We have cross-matched their catalogue with the one in Jackson et al. (2021, their Tables 3 and A2). There are 9395 stars with valid membership probabilities measured in both catalogues[13]; Fig. 6 shows the difference in membership probability. This difference has a peak near zero, with an average value of −0.12 (rms = 0.27). For 50% of the stars the difference is within ±0.1 and for more than 75% is within ±0.3 (4791 and 7306 stars over 9395 in total, respectively).

More in depth comparisons with previous results and membership determination using other methods are presented in Jackson et al. (2020, 2021). In particular, a discussion of the merit of using also RV in addition to proper motions (and parallax) to define membership can be found there. Very briefly, by adding the *Gaia*-ESO RVs, the fraction of false positives is efficiently reduced, meaning that a better separation of cluster members from the surrounding field can be reached. This is especially true for clusters at larger distances.

A summary of the results is given in Table A.1, where the clusters are ordered by ascending age. The fractions shown in the table should not be directly compared to the values in Table 5, as only part of the observed targets could be used in the fit (see original paper for details).

7. Summary

An observational project such as the *Gaia*-ESO Survey, employing 340 VLT nights over six years, required careful selection of targets to maximise the effectiveness of the observational planning and ensure success in achieving its scientific objectives. We eventually observed 62 OCs and SFRs, see the list in Table A.1, and Randich et al. (2021) for details.

The *Gaia*-ESO consortium is organised in working groups specialised in different tasks following a clear work-flow (Gilmore et al. 2012, Randich et al. 2013). In this paper, we described how three of these working groups prepared the actual observations. We focused, in particular, on the crucial task of selecting the target stars for each cluster which would grant

[13] Note that γ Vel is indicated as Pozzo 1 and λ Ori as Collinder 69 in Cantat-Gaudin et al. (2018).

Table 6. Example of candidate members observed and available in a few clusters.

Cluster	N GES observed	N GES $G \leq 18$	N C-T $d \leq 12.5'$	N C-T prob ≥ 0.7	N C-T prob ≥ 0.9	Members J+2021	GES/C-T prob ≥ 0.7	GES/C-T prob ≥ 0.9
NGC 6709	730	664	223	158	76	125	0.79	1.64
NGC 6705	1066	1012	2439	883	245	526	0.60	2.15
NGC 6802	197	183	753	270	100	55	0.20	0.55
NGC 2355	208	190	314	222	88	139	0.63	1.58
NGC 2158	616	490	1633	1186	647	346	0.29	0.53
NGC 2420	562	509	513	331	121	384	1.16	3.17
NGC 2243	710	521	531	479	327	538	1.12	1.65
Berkeley 39	899	675	562	508	382	507	1.00	1.33
Berkeley 36	739	356	374	112	51	212	1.89	4.16

Notes. N GES is the number of stars in *Gaia*-ESO final data release; C-T stands for Cantat-Gaudin et al. (2018), Cantat-Gaudin & Anders (2020); J+21 stands for Jackson et al. (2021), their Tables 4, 5; the last two columns give the fractions of stars assumed as member by J+21 and C-T (for the latter, membership probability larger than 0.7 and 0.9 were selected.

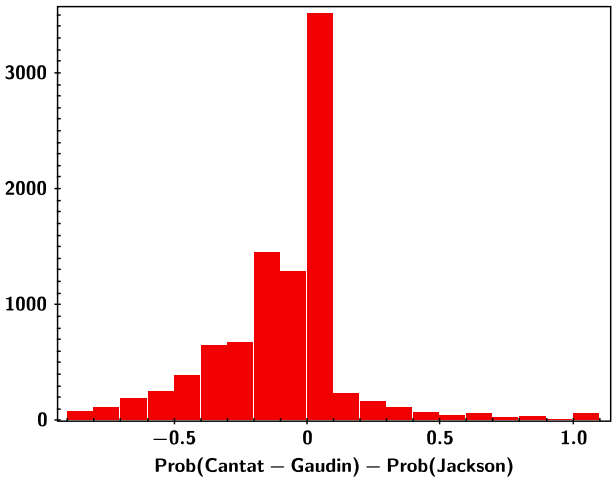

Fig. 6. Histogram of the difference in membership probability measured by Cantat-Gaudin et al. (2018), Cantat-Gaudin & Anders (2020), and Jackson et al. (2021).

reaching the survey main goals, generating at the same time the largest, more accurate, and more homogeneous spectroscopic data set on star clusters ever achieved.

Gaia-ESO is an ESO legacy project: the survey, especially when combined with the *Gaia* results, has a strong impact on the astronomical community. The raw data are fully available without proprietary time and *Gaia*-ESO is also providing advanced data products (reduced spectra, photometry, stellar parameters, etc) that can be the basis for future studies, likely with scientific goals different from the ones driving the survey. To fully exploit this archive, future users must be aware of the complete process that generated the data. One of the key steps is the choice of the stars targeted in the many clusters.

Given the diversity of cutting-edge astronomical problems that can be addressed through the analysis of star clusters and their very different properties in terms of brightness and spectral types distribution, angular size, surface density, richness, etc., the design of a single selection procedure applicable to all clusters is an impossible task. However, we believe that there are some common patterns that underlie all cases and define the backbone of the procedure described in Sects. 4 and 5. In particular, we stressed our decision to be as inclusive and unbiased as possible in our selection of targets, and to discard only the clear outliers (kinematic or photometric).

The CMDs, both in optical and NIR ranges, formed the primary basis for the selection of candidate targets, according to the fiducial evolutionary lines. In addition, we tried, as far as possible, to use the available kinematic information to eliminate secure non-members. However, this is conditioned by the physical characteristics of the clusters and the existence of prior membership studies, making it impossible to generalise to the entire sample. Only about 40% of the clusters observed included kinematic analysis for the selection of targets. As a good example of our protocol when kinematic selection was possible, we described in some detail its application to the intermediate-age, rich cluster NGC 6705.

The last step before observations consisted in the preparation of the OBs, allocating the FLAMES fibres to the targets. The effectiveness and completeness of the fibres' allocation process depend on many factors (area covered by the cluster, richness, concentration, and magnitude of the targets) but in all cases we observed a significant fraction of all possible targets.

The *Gaia*-ESO spectra are the first kinematic data for many clusters in the survey. They represent an increase of one or two orders of magnitude in the number of cluster stars even for the clusters previously studied. The *Gaia*-ESO data for stellar clusters will have a strong legacy also for combination with future ground-based surveys, both spectroscopic (e.g., WEAVE, 4MOST) or photometric (e.g., LSST at the *Rubin* telescope).

Acknowledgements. We have made use of the WEBDA database, originally developed by J-C. Mermilliod, now operated at the Department of Theoretical Physics and Astrophysics of the Masaryk University. A.B. thanks P. Montegriffo for his software CataPack. This research has made use of the SIMBAD database (Wenger 2000), operated at CDS, Strasbourg, France and of the VizieR catalogue access tool, CDS, Strasbourg, France (DOI: 10.26093/cds/vizier). The original description of the VizieR service was published in Ochsenbein et al. (2000). This research has made use of NASA's Astrophysics Data System. We made extensive use of TOPCAT (`http://www.starlink.ac.uk/topcat/`, Taylor 2005). We benefited from discussions in various *Gaia*-ESO workshops supported by the ESF (European Science Foundation) through the GREAT (*Gaia* Research for European Astronomy Training) Research Network Program. This work has made use of data from the European Space Agency (ESA) mission *Gaia* (`https://www.cosmos.esa.int/gaia`), processed by the *Gaia* Data Processing and Analysis Consortium (DPAC, `https://www.cosmos.esa.int/web/gaia/dpac/consortium`). Funding for the DPAC has been provided by national institutions, in particular the institutions participating in the *Gaia* Multilateral Agreement. We acknowledge the support from INAF and Ministero dell'Istruzione, dell'Università e della Ricerca (MIUR) in the form of the grants 'Premiale VLT 2012' and 'The Chemical and Dynamical Evolution of the Milky

Way and Local Group Galaxies' (prot. 2010LY5N2T). E.J.A. acknowledges the financial support by the Spanish Ministerio de Educacion y Ciencia, through grant AYA2010-17631, and by the Consejeria de Educacion y Ciencia de la Junta de Andalucia, through TIC101 and P08-TIC-4075. This work was partially supported by the *Gaia* Research for European Astronomy Training (GREAT-ITN) Marie Curie network, funded through the European Union Seventh Framework Programme [FP7/2007-2013] under grant agreement no 264895. This work was partly supported by the European Union FP7 programme through ERC grant no 320360. This work was partly supported by the Leverhulme Trust through grant RPG-2012-541. T.B. was funded by grant No. 621-2009-3911 and grant No. 2018-0485 from The Swedish Research Council. E.J.A. also acknowledges ESF GREAT grant No 6901. R.S. acknowledges support from the National Science Centre, Poland (2014/15/B/ST9/03981). U.H. acknowledges support from the Swedish National Space Agency (SNSA/Rymdstyrelsen). F.J.E. acknowledges financial support from the Spanish MINECO/FEDER through the grant AYA2017-84089 and MDM-2017-0737 at Centro de Astrobiología (CSIC-INTA), Unidad de Excelencia Maria de Maeztu, and from the European Union's Horizon 2020 research and innovation programme under Grant Agreement no. 824064 through the ESCAPE – The European Science Cluster of Astronomy & Particle Physics ESFRI Research Infrastructures project.

References

Baume, G., Vázquez, R. A., Carraro, G., & Feinstein, A. 2003, A&A, 402, 549
Bell, C. P. M., Naylor, T., Mayne, N. J., et al. 2013, MNRAS, 434, 806
Blomme, R., Daflon, S., Gebran, M., et al. 2022, A&A, in press https://doi.org/10.1051/0004-6361/202142349
Bonito, R., Prisinzano, L., Venuti, L., et al. 2020, A&A, 642, A56
Bravi, L., Zari, E., Sacco, G. G., et al. 2018, A&A, 615, A37
Bressan, A., Marigo, P., Girardi, L., et al. 2012, MNRAS, 427, 127
Cantat-Gaudin, T., & Anders, F. 2020, A&A, 633, A99
Cantat-Gaudin, T., Vallenari, A., Zaggia, S., et al. 2014, A&A, 569, A17
Cantat-Gaudin, T., Jordi, C., Vallenari, A., et al. 2018, A&A, 618, A93
Cantat-Gaudin, T., Anders, F., Castro-Ginard, A., et al. 2020, A&A, 640, A1
Carraro, G., Patat, F., & Baumgardt, H. 2001, A&A, 371, 107
Carraro, G., Costa, E., & Ahumada, J. A. 2010, AJ, 140, 954
Castro-Ginard, A., Jordi, C., Luri, X., et al. 2020, A&A, 635, A45
Daflon, S., & Cunha, K. 2004, ApJ, 617, 1115
Damiani, F., Klutsch, A., Jeffries, R. D., et al. 2017, A&A, 603, A81
Delgado, A. J., Alfaro, E. J., & Yun, J. L. 2007, A&A, 467, 1397
Delgado, A. J., Sampedro, L., Alfaro, E. J., et al. 2016, MNRAS, 460, 3305
Donati, P., Cantat Gaudin, T., Bragaglia, A., et al. 2014a, A&A, 561, A94
Donati, P., Beccari, G., Bragaglia, A., et al. 2014b, MNRAS, 437, 1241
Drew, J. E., Greimel, R., Irwin, M. J., et al. 2005, MNRAS, 362, 753
Drew, J. E., Gonzalez-Solares, E., Greimel, R., et al. 2014, MNRAS, 440, 2036
Favata, F., & Micela, G. 2003, Space Sci. Rev., 108, 577
Feigelson, E., Townsley, L., Güdel, M., & Stassun, K. 2007, in Protostars and Planets V, eds. B. Reipurth, D. Jewitt, & K. Keil, 313
Franciosini, E., Tognelli, E., Degl'Innocenti, S., et al. 2022, A&A, 659, A85
Friel, E. D. 1995, ARA&A, 33, 381
Friel, E. D., Donati, P., Bragaglia, A., et al. 2014, A&A, 563, A117
Frinchaboy, P. M., & Majewski, S. R. 2008, AJ, 136, 118
Gaia Collaboration (Prusti, T., et al.) 2016a, A&A, 595, A1
Gaia Collaboration (Brown, A. G. A., et al.) 2016b, A&A, 595, A2
Gaia Collaboration (van Leeuwen, F., et al.) 2017, A&A, 601, A19
Gaia Collaboration (Brown, A. G. A., et al.) 2018a, A&A, 616, A1
Gaia Collaboration (Babusiaux, C., et al.) 2018b, A&A, 616, A10
Gaia Collaboration (Brown, A. G. A., et al.) 2021, A&A, 649, A21
Galli, P. A. B., Bouy, H., Olivares, J., et al. 2021, A&A, 646, A46
Gieles, M., Portegies Zwart, S. F., Baumgardt, H., et al. 2006, MNRAS, 371, 793
Gilmore, G., Randich, S., Asplund, M., et al. 2012, Messenger, 147, 25
Gilmore, G., Randich, S., Worley, C. C., et al. 2021, A&A, submitted
Girard, T. M., van Altena, W. F., Zacharias, N., et al. 2011, AJ, 142, 15
Gonzalez, G., & Wallerstein, G. 2000, PASP, 112, 1081
Grasser, N., Ratzenböck, S., Alves, J., et al. 2021, A&A, 652, A2
Groot, P. J., Verbeek, K., Greimel, R., et al. 2009, MNRAS, 399, 323
Hatzidimitriou, D., Held, E. V., Tognelli, E., et al. 2019, A&A, 626, A90
Hayes, C., & Friel, E. D. 2013, AJ, 147, 69
Jackson, R. J., Jeffries, R. D., Lewis, J., et al. 2015, A&A, 580, A75
Jackson, R. J., Jeffries, R. D., Wright, N. J., et al. 2020, MNRAS, 496, 4791
Jackson, R. J., Jeffries, R. D., Wright, N. J., et al. 2021, MNRAS, 509, 1664
Jadhav, V. V., Pennock, C. M., Subramaniam, A., et al. 2021, MNRAS, 503, 236
Janes, K. A., & Phelps, R. L. 1994, AJ, 108, 1773
Jeffries, R. D., Naylor, T., Walter, F. M., Pozzo, M. P., & Devey, C. R. 2009, MNRAS, 393, 538
Jeffries, R. D., Jackson, R. J., Cottaar, M., et al. 2014, A&A, 563, A94
Keller, S. C., Schmidt, B. P., Bessell, M. S., et al. 2007, PASA, 24, 1
Kharchenko, N. V., Scholz, R.-D., Piskunov, A. E., Röser, S., & Schilbach, E. 2007, Astron. Nachr., 328, 889
Koo, J.-R., Kim, S.-L., Rey, S.-C., et al. 2007, PASP, 119, 1233
Lada, C. J., & Lada, E. A. 2003, ARA&A, 41, 57
Lindegren, L., Hernández, J., Bombrun, A., et al. 2018, A&A, 616, A2
Liu, L., & Pang, X. 2019, ApJS, 245, 32
Lovis, C., & Mayor, M. 2007, A&A, 472, 657
Magrini, L., Randich, S., Donati, P., et al. 2015, A&A, 580, A85
Magrini, L., Lagarde, N., Charbonnel, C., et al. 2021, A&A, 651, A84
McMahon, R. 2012, Science from the Next Generation Imaging and Spectroscopic Surveys
Mermilliod, J. C., Mayor, M., & Udry, S. 2008, A&A, 485, 303
Mignard, F. 2005, in Astrometry in the Age of the Next Generation of Large Telescopes, ASP Conf. Ser., 338, 15
Ochsenbein, F., Bauer, P., & Marcout, J. 2000, A&AS, 143, 23
Overbeek, J. C., Friel, E. D., Donati, P., et al. 2017, A&A, 598, A68
Pancino, E., Lardo, C., Altavilla, G., et al. 2017, A&A, 598, A5
Pasquini, L., Avila, G., Blecha, A., et al. 2002, Messenger, 110, 1
Prisinzano, L., Damiani, F., Micela, G., et al. 2016, A&A, 589, A70
Prisinzano, L., Damiani, F., Kalari, V., et al. 2019, A&A, 623, A159
Randich, S., Gilmore, G., & Gaia-ESO Consortium 2013, Messenger, 154, 47
Randich, S., Tognelli, E., Jackson, R., et al. 2018, A&A, 612, A99
Randich, S., Gilmore, G., Magrini, L., et al. 2021, A&A, submitted
Rigliaco, E., Wilking, B., Meyer, M. R., et al. 2016, A&A, 588, A123
Romano, D., Magrini, L., Randich, S., et al. 2021, A&A, 653, A72
Röser, S., Schilbach, E., Schwan, H., et al. 2008, A&A, 488, 401
Sacco, G. G., Spina, L., Randich, S., et al. 2017, A&A, 601, A97
Sartoretti, P., Katz, D., Cropper, M., et al. 2018, A&A, 616, A6
Semenova, E., Bergemann, M., Deal, M., et al. 2020, A&A, 643, A164
Siess, L., Dufour, E., & Forestini, M. 2000, A&A, 358, 593
Sim, G., Lee, S. H., Ann, H. B., et al. 2019, J. Korean Astron. Soc., 52, 145
Skrutskie, M. F., Cutri, R. M., Stiening, R., et al. 2006, AJ, 131, 1163
Soubiran, C., Cantat-Gaudin, T., Romero-Gómez, M., et al. 2018, A&A, 619, A155
Spina, L., Randich, S., Palla, F., et al. 2014, A&A, 567, AA55
Sung, H., Bessell, M. S., Lee, H.-W., Kang, Y. H., & Lee, S.-W. 1999, MNRAS, 310, 982
Tang, B., Geisler, D., Friel, E., et al. 2017, A&A, 601, A56
Taylor, M. B. 2005, in Astronomical Data Analysis Software and Systems XIV, ASP Conf. Ser., 347, 29
Venuti, L., Prisinzano, L., Sacco, G. G., et al. 2018, A&A, 609, A10
Wenger, M., et al. 2000, A&AS, 143, 9
Wright, N. J., Jeffries, R. D., Jackson, R. J., et al. 2019, MNRAS, 486, 2477
Zacharias, N., Finch, C. T., Girard, T. M., et al. 2013, AJ, 145, 44

[1] INAF–Osservatorio di Astrofisica e Scienza dello Spazio di Bologna, via P. Gobetti 93/3, 40129 Bologna, Italy
e-mail: angela.bragaglia@inaf.it
[2] Instituto de Astrofísica de Andalucía-CSIC, Apdo. 3004, 18080 Granada, Spain
[3] INAF–Osservatorio Astronomico di Palermo, Piazza del Parlamento 1, 90134 Palermo, Italy
[4] Royal Observatory of Belgium, Ringlaan 3, 1180 Brussels, Belgium
[5] University of Cádiz, Cádiz, Spain
[6] INAF–Osservatorio Astrofisico di Arcetri, Largo E. Fermi, 5, 50125 Firenze, Italy
[7] Department of Astronomy, Indiana University, Bloomington, USA
[8] Section of Astrophysics, Astronomy and Mechanics, Department of Physics, National and Kapodistrian University of Athens, 15784 Athens, Greece
[9] INAF–Osservatorio Astronomico di Padova, Vicolo Osservatorio 5, 35122 Padova, Italy
[10] INAF–Osservatorio Astrofisico di Torino, Via Osservatorio 20, 10025 Torino, Italy
[11] Institut de Ciències del Cosmos, Universitat de Barcelona (IEEC-ICCUB), Martí i Franquès 1, 08028 Barcelona, Spain
[12] Laboratoire d'Astrophysique de Bordeaux, Univ. Bordeaux, CNRS, B18N, allée Geoffroy Saint-Hilaire, 33615 Pessac, France
[13] Astrophysics Group, Research Institute for the Environment, Physical Sciences and Applied Mathematics, Keele University, Keele, Staffordshire ST5 5BG, UK

[14] Dept. Física Quàntica i Astrofísica, Institut de Ciències del Cosmos (ICCUB), Universitat de Barcelona (IEEC-UB), Martí Franquès 1, 08028 Barcelona, Spain
[15] Centre for Astrophysics Research, STRI, University of Hertfordshire, College Lane Campus, Hatfield AL10 9AB, UK
[16] Institut für Astronomie und Astrophysik Tübingen (IAAT), Sand 1, 72076, Tübingen, Germany
[17] Department of Astronomy, University of Washington, Box 351580, Seattle, WA 98195, USA
[18] Departamento de Astrofísica, Centro de Astrobiología (CSIC-INTA), ESAC Campus, Camino Bajo del Castillo s/n, 28692 Villanueva de la Cañada, Madrid, Spain
[19] Instituto de Física y Astronomía, Facultad de Ciencias, Universidad de Valparaíso, Av. Gran Bretaña 1111, 5030 Casilla, Valparaíso, Chile
[20] Lund Observatory, Department of Astronomy and Theoretical Physics, Box 43, 221 00 Lund, Sweden
[21] Max-Planck Institut für Astronomie, Königstuhl 17, 69117 Heidelberg, Germany
[22] Institute of Astronomy, University of Cambridge, Madingley Road, Cambridge CB3 0HA, UK
[23] Observational Astrophysics, Division of Astronomy and Space Physics, Department of Physics and Astronomy, Uppsala University, Box 516, 751 20 Uppsala, Sweden
[24] Space Science Data Center – Agenzia Spaziale Italiana, via del Politecnico, s.n.c., 00133 Roma, Italy
[25] Nicolaus Copernicus Astronomical Center, Polish Academy of Sciences, ul. Bartycka 18, 00-716 Warsaw, Poland
[26] Armagh Observatory and Planetarium, College Hill, BT61 9DG Armagh, Northern Ireland, UK

Appendix A: Open clusters observed by GES

Figure A.1 shows the Galactic positions of all OCs observed by *Gaia*-ESO. Table A.1 gives the complete list of names in ascending age order and information on them. Three clusters are separated from the main list: M67 and NGC 6253 were observed as calibrators and their selection of targets is not the same of the main sample; Loden 165 has not been confirmed as a genuine open cluster (its coordinates and age come from Carraro et al. 2001).

Equatorial coordinates and ages come from Cantat-Gaudin et al. (2020) as in Randich et al. (2021), except for the ages of NGC 2244, NGC 6530 (Bell et al. 2013); NGC 2264 (Venuti et al. 2018); γ Vel (Franciosini et al. 2022); Trumpler 14 (Damiani et al. 2017); ρ Oph (Grasser et al. 2021); and Chamaleon I (Galli et al. 2021). The column Class indicates the class, as defined in Sects 2 and 3: 1a is for young OCs, with no or few massive stars, 1b is for massive-star young clusters, and 2 is for older clusters. Metallicity based on GES published papers is indicated in column [Fe/H], taken from Randich et al. (2021); for NGC 3293, NGC 3766, and NGC 6649 values come from unpublished iDR6 results. Information on membership comes from Jackson et al. (2021, Tables 1, 2, 4, and 5) and is available for almost all clusters. We note that N_{obs} is the number of targets observed in each cluster with UVES and GIRAFFE HR15n (the main sample analysed by Jackson et al. 2021); N_{comp} is the number of targets with a full set of the required data (2MASS K_s, *Gaia* G, *Gaia*-ESO T_{eff}, and S/N>5, see their Sect. 2); N_{fit} is the number of targets actually fitted in the membership analysis. Fractio M is the fraction of the N_{fit} targets analysed and with a valid membership probability (i.e. not -1 in their Table 3) that are expected to be cluster members. In a few cases, these four values are absent in Jackson et al. (2021).

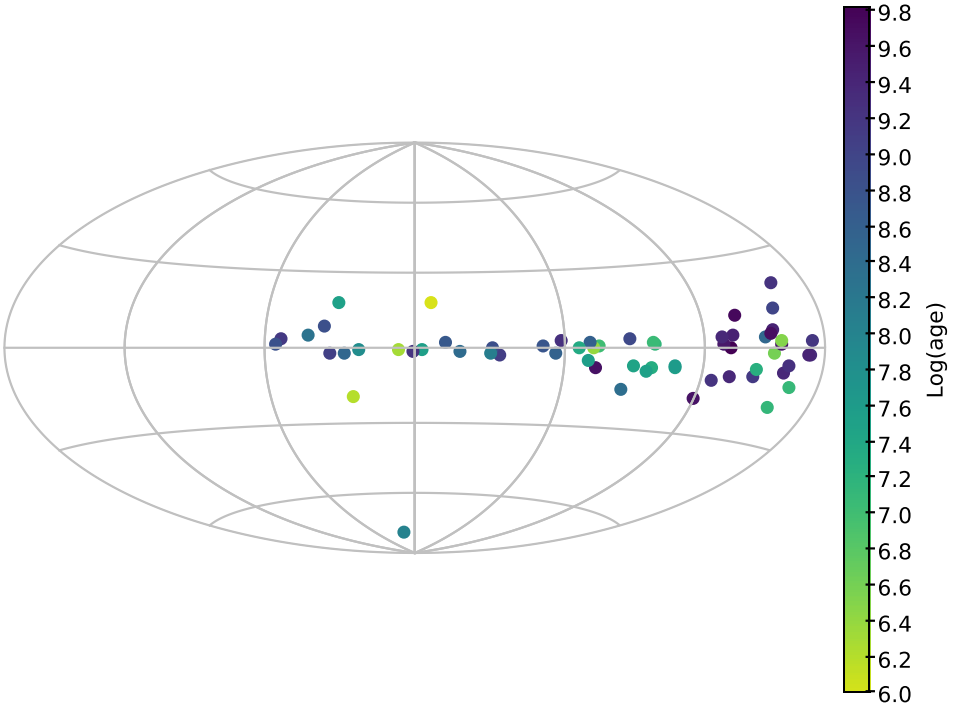

Fig. A.1. Plot of all objects observed by GES in Galactic coordinates. The clusters are colour-coded by their age.

Table A.1. Information on the *Gaia*-ESO observed clusters.

Cluster	RA (J2000)	Dec (J2000)	age (Gyr)	Class	[Fe/H]	N_{obs}	N_{comp}	N_{fit}	Fractio M
ρ Oph	16:24:00.00	-23:48:00.0	0.001	1a	0.03	311	301	72	0.63
Chamaeleon I	16:24:00.00	-23:48:00.0	0.001	1a	-0.03	708	687	170	0.55
NGC 6530	18:04:21.60	-24:19:48.0	0.002	1b	-0.02	1972	1907	1501	0.34
Trumpler 14	10:43:56.64	-59:33:10.8	0.003	1b	-0.01	1111	1069	741	0.53
NGC 2264	06:40:52.08	+09:52:37.2	0.003	1b	-0.10	1876	1819	1408	0.38
NGC 2244	06:32:10.80	+04:54:50.4	0.004	1b	-0.04	432	427	375	0.35
NGC 3293	10:35:52.80	-58:13:51.6	0.010	1b	-0.08				
ASCC 50/Alessi 43	08:50:31.44	-41:44:16.8	0.011	1a	0.02	1224	1192	501	0.41
Collinder 69/λ Ori	05:35:10.08	+09:48:46.8	0.013	1a	-0.09	608	588	344	0.60
25 Ori	05:24:47.52	+01:39:18.0	0.013	1a	0.00	294	284	256	0.68
Collinder 197	08:44:48.48	-41:16:48.0	0.014	1a	0.03	409	395	334	0.37
NGC 2232	06:27:33.12	-04:44:56.4	0.018	1a	-0.03	1761	1734	697	0.13
γ Vel	08:09:29.76	-47:20:06.0	0.020	1a	-0.02	1262	1242	497	0.45
NGC 3766	11:36:14.64	-61:36:57.6	0.023	1b	-0.12				
IC 2391	08:41:10.08	-52:59:27.6	0.029	1a	-0.06	434	426	78	0.61
NGC 2547	08:10:06.00	-49:11:52.8	0.032	1a	-0.03	477	472	269	0.62
IC 4665	17:46:12.96	+05:36:54.0	0.033	1a	0.01	567	562	298	0.11
NGC 6405	17:40:16.56	-32:14:31.2	0.035	1a	-0.02	659	654	373	0.19
NGC 2451A	07:42:56.64	-38:15:50.4	0.035	1a	-0.08	1656	1637	352	0.13
IC 2602	10:42:27.12	-64:25:33.6	0.036	1a	-0.06	1840	1817	117	0.53
NGC 2451B	07:44:30.72	-37:57:14.4	0.041	1a	-0.02	1656	1635	425	0.16
NGC 6649	18:33:26.16	-10:23:56.4	0.071	1b	-0.08	122	121	116	0.62
Blanco 1	00:03:24.72	-29:57:28.8	0.105	2	-0.03	463	446	314	0.43
NGC 6067	16:13:11.76	-54:13:37.2	0.126	2	0.03	532	531	512	0.39
NGC 6709	18:51:20.64	+10:20:02.4	0.191	2	-0.02	684	681	551	0.15
NGC 2516	07:58:06.48	-60:48:00.0	0.240	2	-0.04	759	745	641	0.75
NGC 6259	17:00:46.80	-44:40:40.8	0.269	2	0.18	438	423	391	0.38
Berkeley 30	06:57:45.12	+03:13:44.4	0.295	2	-0.13	226	224	216	0.34
NGC 6705	18:51:03.84	-06:16:19.2	0.309	2	0.03	1066	1042	977	0.59
NGC 4815	12:57:59.76	-64:57:36.0	0.372	2	0.08	126	126	112	0.50
NGC 3532	11:05:40.08	-58:42:25.2	0.398	2	-0.01	966	952	687	0.73
NGC 6281	17:04:42.96	-37:56:52.8	0.513	2	-0.04	251	249	63	0.44
Pismis 18	13:36:54.48	-62:05:27.6	0.575	2	0.14	101	101	90	0.31
NGC 6802	19:30:36.24	+20:15:43.2	0.661	2	0.14	103	103	98	0.56
NGC 6633	18:27:22.80	+06:36:54.0	0.692	2	-0.03	1595	363	119	0.21
Trumpler 23	16:00:52.32	-53:32:20.4	0.708	2	0.20	89	89	83	0.47
Pismis 15	09:34:44.16	-48:02:24.0	0.871	2	0.02	235	235	224	0.19
NGC 2355	07:16:59.28	+13:46:19.2	1.000	2	-0.13	208	208	204	0.69
Berkeley 81	19:01:40.56	-00:27:14.4	1.148	2	0.22	203	203	171	0.34
NGC 6005	15:55:49.20	-57:26:20.4	1.259	2	0.22	355	353	325	0.19
Berkeley 73	06:22:04.80	-06:19:15.6	1.413	2	-0.26	76	75	70	0.66
Berkeley 44	19:17:15.12	+19:33:00.0	1.445	2	0.22	93	92	83	0.51
NGC 2158	06:07:26.88	+24:05:56.4	1.549	2	-0.15	616	598	571	0.67
Ruprecht 134	17:52:44.16	-29:32:13.2	1.660	2	0.27	680	665	602	0.18
NGC 2420	06:49:00.48	-23:59:56.4	1.698	2	-0.15	562	557	520	0.75
Berkeley 75	07:38:24.48	+21:34:30.0	1.738	2	-0.34	75	74	64	0.71
NGC 2141	06:02:56.16	+10:27:03.6	1.862	2	-0.04	853	846	801	0.76
Trumpler 20	12:39:31.68	-60:38:13.2	1.862	2	0.13	552	545	490	0.38
Berkeley 21	05:51:43.20	+21:48:43.2	2.138	2	-0.21	744	738	574	0.34
NGC 2425	07:38:18.48	-14:53:06.0	2.399	2	-0.13	528	525	481	0.31
Berkeley 22	05:58:28.32	+07:45:46.8	2.455	2	-0.26	395	395	352	0.52
Berkeley 25	06:41:16.08	-16:29:13.2	2.455	2	-0.25				
Czernik 24	05:55:23.52	+20:52:33.6	2.692	2	-0.11	346	343	302	0.27
Berkeley 31	06:57:37.44	+08:17:06.0	2.818	2	-0.29	616	614	499	0.34
Czernik 30	07:31:11.04	-09:56:42.0	2.884	2	-0.31	226	226	193	0.38
Haffner 10	07:28:37.44	-15:21:50.4	3.802	2	-0.10	460	457	428	0.62
Trumpler 5	06:36:30.24	+09:27:54.0	4.266	2	-0.35	1138	1132	1098	0.76
NGC 2243	06:29:34.80	-31:16:55.2	4.365	2	-0.45	703	701	614	0.88
ESO 92-05	10:03:12.24	-64:45:18.0	4.467	2	-0.29	212	210	114	0.80
Berkeley 32	06:58:07.20	+06:25:58.8	4.898	2	-0.31	389	385	348	0.70
Berkeley 39	07:46:48.48	-04:39:54.0	5.623	2	-0.14	899	897	832	0.62
Berkeley 36	07:16:25.20	-13:11:45.6	6.761	2	-0.15	739	737	672	0.34
Messier 67	08:51:23.04	+11:48:50.4	3.981	-	-0.02	131	131	130	0.92
NGC 6253	16:59:06.72	-52:42:43.2	3.246	-	0.33	294	235	227	0.72
Loden 165	10:35:56	-58:44:03	3	2		388	387	333	